PROCEEDINGS OF SCIENCE

Between the cosmic-ray 'knee' and the 'ankle': Contribution from star clusters

Sourav Bhadra,[a,b,*] **Satyendra Thoudam,**[c] **Biman Nath**[a] **and Prateek Sharma**[b]

[a] *Raman Research Institute, Sadashiva Nagar, Bangalore 560080, India*
[b] *Department of Physics, Indian Institute of Science, Bangalore 560012, India*
[c] *Department of Physics, Khalifa University, PO Box 127788, Abu Dhabi, United Arab Emirates*

E-mail: souravbhadra@iisc.ac.in, sbhadra@rri.res.in

It is believed that Cosmic Rays (CRs) up to PeV (10^6 GeV) are accelerated by supernova shocks, and extra-Galactic CR contribution dominates in the range above $\sim 10^9$ GeV. Therefore, some other yet unknown sources must act as sources for the CR spectrum in between. Our recent work shows that stellar winds from massive young star clusters can explain Galactic CRs in the intermediate range. The wind termination shock (WTS) in these star clusters is strong enough to accelerate particles in this energy range, which is difficult to reach in the standard paradigm of CR acceleration in supernova remnants. We present a model for producing different nuclei in CRs from massive stellar winds using the observed spatial distribution of young star clusters in the Galactic plane and the elemental abundances in the stellar wind. We present a detailed calculation of CR transport in the Galaxy, considering the effect of diffusion, interaction losses, and re-acceleration by older supernova remnants to determine the all-particle CR spectrum. Using the estimated magnetic field values instar clusters, we argue the WTS can accelerate protons up to a few tens of PeV. To match the observations with our model, an exponential energy cutoff of $(60-70)\times Z$ PeV and a cosmic-ray injection fraction of $\sim (5-6)\%$ from the clusters are needed. We, therefore, argue that this CR component originating from star clusters is the natural 'second component' of Galactic cosmic rays.

38th International Cosmic Ray Conference (ICRC2023)
26 July - 3 August 2023
Nagoya, Japan

*Speaker

© Copyright owned by the author(s) under the terms of the Creative Commons Attribution-NonCommercial-NoDerivatives 4.0 International License (CC BY-NC-ND 4.0).

PoS(ICRC2023)196

1. Introduction

The diffusive shock acceleration (DSA) mechanism is thought to be responsible for the acceleration of lower energy cosmic rays (CRs hereafter), up to 10^{5-6} GeV [1, 2]. This process occurs when supernova shocks accelerate the cosmic rays, and $\sim 10\%$ of the shock energy is expected to be converted into cosmic rays. On the other hand, cosmic rays above approximately 10^9 GeV are believed to originate from extra-galactic sources such as galaxy clusters[3], radio galaxies[4], AGN jets[5], or gamma-ray bursts[6]. However, there exists a region between approximately 10^7 and 10^9 GeV, referred to as the region between 'knee' and 'ankle', where the contribution from supernova shocks and the extra-galactic component is small, and therefore there remains a gap.

In recent times, the acceleration of cosmic rays to extremely high energies in massive star clusters has been supported by γ-ray observations conducted by LHAASO, HESS, Fermi-LAT, and HAWC. These observations have provided evidence of CR acceleration occurring in a few massive star clusters, such as Westerlund1 and Cygnus [7, 8]. Therefore, these star-forming regions have been discussed as potential candidates for CR accelerators [9]. Recently, Gupta et al. [10] has shown that the excess (^{22}Ne/^{20}Ne) ratio can be explained by considering wind termination shock (WTS) of massive star clusters as CR accelerators. Additionally, Tatischeff et al. [11] showed that the refractory elements of Galactic cosmic rays are produced in super-bubbles. This combination of theoretical and observational evidence has prompted us to investigate the overall contribution of cosmic rays originating from the distribution of massive star clusters in our Galaxy.

Star clusters, the birth sites of massive stars that eventually undergo supernova explosions, exhibit a continuous outflow of mass through stellar winds. These clusters are primarily found in dense molecular clouds and possess a considerable mass on the order of several thousand solar masses [12]. Star clusters host massive stars as well as supernova explosions, which produce a low-density bubble around them [13, 15]. We will show below that, young star clusters contain sufficient kinetic energy supplied by interacting stellar winds, which can accelerate protons up to a few times 10^7 GeV. This cosmic ray component originating from star clusters can be considered as the second component of Galactic cosmic rays, which can explain the observed all-particle spectra in the energy range of $10^7 - 10^9$ GeV of cosmic rays.

2. The second component of Galactic cosmic rays

In this work, we discuss one potential scenario of the Galactic component of CRs: the acceleration of cosmic rays by the young massive star clusters, which we briefly mentioned in the Introduction. There has been particular speculation that the winds emanating from massive stars could serve as suitable sites for CR acceleration [14–16]. CRs accelerated at the WTS of young star clusters with age $\leq$ 10 Myr can make a significant contribution to the overall observed flux of CRs [10]. Notably, the recent observations by LHAASO have detected γ-rays in the PeV energy range from young massive star clusters [17], which can be associated with cosmic ray acceleration in those clusters.

PoS(ICRC2023)196

2.1 Transport of CRs and the distribution of star clusters in the Galaxy

After the acceleration in the star cluster, CRs undergo propagation throughout the Galaxy. This propagation is primarily governed by diffusion and energy loss resulting from interaction with ISM material. Some fraction of the propagating CRs can be re-accelerated up to higher energy by the interaction with existing weaker shocks that have been generated from older supernova remnants in the ISM [18]. The transport equation describing the steady-state behavior of CR nuclei can be expressed as:

$$\nabla \cdot (D\nabla N) - [nv\sigma + \zeta]\delta(z)N + \left[\zeta s p^{-s} \int_{p_0}^{p} du\, N(u)\, u^{s-1}\right]\delta(z) = -Q(r,p)\delta(z). \tag{1}$$

The momentum-dependent diffusion coefficient, denoted as $D(p)$, plays a crucial role in cosmic ray (CR) particles. Here $v(p)$ is the CR particle velocity, $\sigma(p)$ is the cross-section of inelastic collision, n represents the averaged surface density of interstellar atoms in the Galaxy, N is the differential number density (number per unit volume per momentum) and ζ is the rate of re-acceleration. The third term within the equation incorporates the momentum integral, which accounts for the generation of higher energy particles resulting from the re-acceleration of lower energy particles. It has been assumed that a CR population is instantaneously re-accelerated to form a power-law distribution with an index of $s \sim 4.5$ [18].

The term on the right side, $Q(r,p)\delta(z)$, signifies the injection rate of cosmic rays per unit volume by the sources. The injection term $Q(r,p)$ can be expressed as a combination of a space-dependent part and a momentum-dependent part, i.e. $Q(r,p) = v(r)\, H[R-r]\, H[p-p_0]\, Q(p)$, where $v(r)$ represents the number of star clusters per unit surface area on the Galactic disk. Our assumed distribution of star clusters, motivated by observations follows a Gaussian pattern, which has a peak at $R_p \sim 4.6$ kpc and then decreases rapidly at large distances [19]. The surface density of the clusters can be approximately written as,

$$v(r) = \Sigma_0\, e^{\frac{-(r-R_p)^2}{\sigma^2}} \tag{2}$$

where r is the Galactocentric distance and $\sigma = 3$ kpc and $\Sigma_0 \sim 14$ kpc^{-2} [20] is the normalization constant. Following the procedure described in [18], we get the solution of the transport equation,

$$N(r,p) = \int_{r'=0}^{r} \int_{k=0}^{\infty} \Sigma_0 \frac{J_0[k(r-r')]}{L(p)}\, k\, dk\, e^{-(r'-R_p)^2/\sigma^2}\, r'\, dr'$$
$$\left[Q(p) + \zeta s p^{-s} \int_{p_0}^{p} p'^{s}\, dp'\, Q(p')\, A(p') \times \exp\left(\zeta s \int_{p'}^{p} A(u) du\right)\right], \tag{3}$$

where $L(p) = 2D(p)k\, \coth(kH) + nv\sigma(p) + \zeta$ and $A(p) = 1/pL(P)$.

2.2 Injection spectra and Maximum energy of accelerated particles in star clusters

The CR source spectrum $Q(p)$ from star clusters is assumed to follow a power-law in total momentum Ap, with an exponential cut-off, where A is the mass number of the nucleus. We write the differential number of CR particles with nucleon number A, having momentum per nucleon in the range $(p\,, p+dp)$, as,

$$\frac{dQ(p)}{dp} = Q_0 (Ap)^{-q} \exp\left(-\frac{Ap}{Zp_{\max}}\right). \tag{4}$$

PoS(ICRC2023)196

Here Q_0 serves as a normalization constant that is proportional to the fraction of total wind kinetic energy f converted into cosmic rays by an individual star cluster. We refer to this proportion as the 'injection fraction', which is a free parameter and can be estimated by comparing the model result with observations. Additionally, q is the spectral index, $p_{\rm max}$ is the cutoff momentum (for a single nucleon), and Ap is the total momentum of a particle with the mass number A.

The maximum energy is achieved when the diffusion length of particles becomes comparable to the size of the shock region, for beyond this limit, the particles escape out of the accelerating region. The maximum energy is then [21]:

$$E_{\rm max} \sim \zeta\, q\, B_{\rm WTS}\, \Delta R\, \frac{V_w}{c}\,. \tag{5}$$

Here $B_{\rm WTS}$ is the value of the magnetic field at the WTS position, V_w is the velocity of stellar wind, ΔR is the size of the accelerating region, which in our case is the width of the shocked wind region. This estimation is based on the Hillas criteria [22], and $\zeta = 3r_g/\lambda$ (considering Bohm diffusion), with λ the mean free path due to the magnetic field.

Using the arguments advocated by Vieu et al. 2022 [21] to estimate the magnetic field in the cluster core, we found the maximum accelerated energy can be written as,

$$E_{\rm max} \sim 31 \left(\frac{\zeta}{3}\right) \left(\frac{n_{\rm amb}}{10\,{\rm cm^{-3}}}\right)^{1/6} \left(\frac{\eta_T}{0.2}\right)^{1/3} \left(\frac{N_{\rm OB}}{1000}\right)^{2/9} \left(\frac{\Delta R/R_{\rm WTS}}{5}\right) \left(\frac{R_c}{1\,{\rm pc}}\right)^{1/3} \left(\frac{v_w}{2000\,{\rm km\,s^{-1}}}\right) \text{ PeV}. \tag{6}$$

Equation 6 provides a conservative estimate of $\rm E_{max}$ = 31 PeV (3.1×10^7 GeV) as the maximum achievable energy for protons within the shocked wind region. Note that, this estimate exceeds the maximum energy observed in the SNR acceleration scenario by at least one order of magnitude. However, it is important to acknowledge that our assumption of a uniform magnetic field throughout the shocked wind region may not hold in realistic scenarios. Turbulence within the region can also lead to an amplified magnetic field, potentially increasing the estimated maximum energy. There may be other uncertainties as well (e.g., the efficiency of generation of turbulence η_T, wind velocity v_w) that can increase the maximum energy by a factor of a few.

3. Model prediction for the second component of galactic cosmic rays

The determination of cosmic ray (CR) propagation parameters and re-acceleration parameters involved a comparison between the observed Boron to Carbon abundance ratio and the corresponding value obtained from the adopted model [18]. The matter density (n), and size of diffusion halo (H) are the same as mentioned in this model [18]. Since our focus is on CR acceleration within the wind termination shock (WTS), the relevant abundances correspond to that in the stellar wind for massive stars. We have used the surface abundance of massive stars as a function of time, calculated after properly taking into account the effect of stellar rotation. Furthermore, the stellar wind elemental abundances are mentioned in Table 1, which are calculated using the method described in Roy et al. 2021 [24].

Figure 1 illustrates the star cluster contribution to CRs. In our analysis, we assume that $\sim 5\%$ of the total kinetic energy of each cluster is channeled into cosmic rays, a fraction determined by fitting the all-particle CR spectrum. The peak for the proton at $\sim 7 \times 10^7$ GeV (70 PeV)

PoS(ICRC2023)196

Elements	q	Fractional abundances in winds
Proton	2.25	0.86
Helium	2.23	0.13
Carbon	2.20	3.32×10^{-3}
Oxygen	2.24	8.51×10^{-4}
Neon	2.24	8.83×10^{-5}
Magnesium	2.28	3.62×10^{-5}
Silicon	2.24	3.42×10^{-5}
Iron	2.24	3.72×10^{-5}

Table 1: Source spectral indices q and fractional abundances of different elements in the wind material. The elemental abundances are calculated following Roy et al. [24].

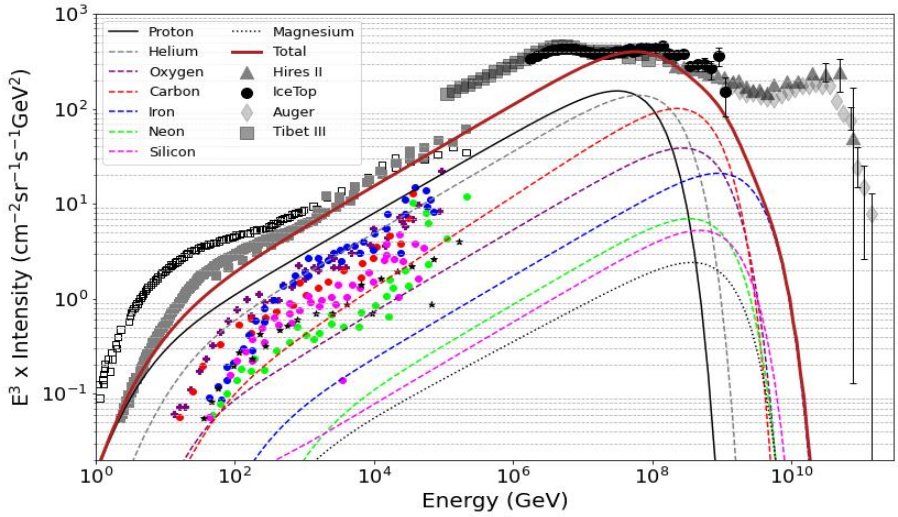

Figure 1: Model prediction for the star cluster model as a second galactic component considering an injection fraction $\sim$ 5%. The thick solid maroon line represents the total contribution from Galactic star clusters. Thin dashed lines represent the flux of individual elements. For the CRs generated from star clusters, an exponential energy cut-off for protons at $E_c = 7 \times 10^7$ GeV (70 PeV) is assumed. High-energy data: IceTop [30], Tibet III [27], the Pierre Auger Observatory [28], and HiRes II [29].

corresponds to the exponential cutoff of the proton source spectrum. This maximum energy value is determined by matching the observed all-particle spectrum with our theoretical prediction. The physical motivation for choosing such a value of maximum energy is mentioned in section 2.2.

4. All-particle spectrum of cosmic rays

Figure 2 presents a comprehensive representation of all three CR components: CRs from supernova shocks (SNR-CR), CRs from star clusters, and extragalactic CRs. The combined spectrum of these components represents the total all-particle spectrum of cosmic rays, which is then compared to various observations. The SNR-CR component shown in this figure is calculated following the methodology outlined in Thoudam et al. 2016 [23]. For the extragalactic component, we have adopted the UFA model [25], which considers a substantial contribution of extragalactic CRs below

PoS(ICRC2023)196

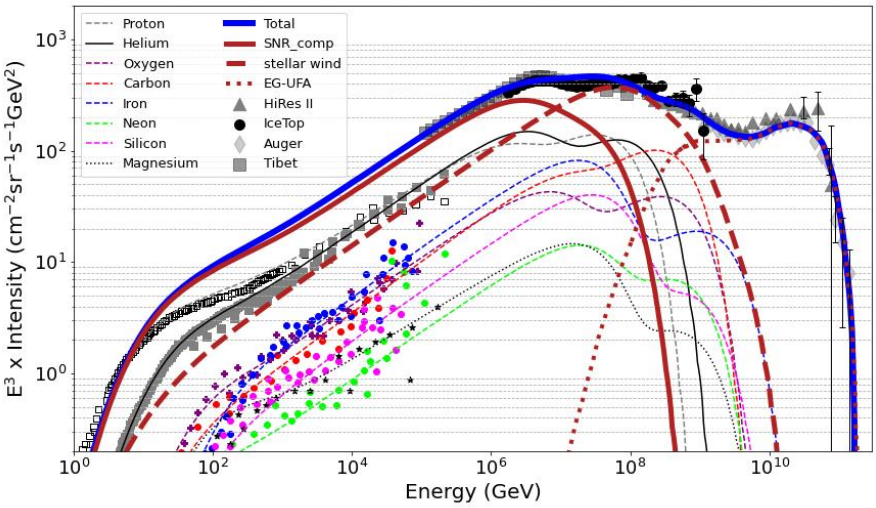

Figure 2: Model prediction for the all-particle spectrum using the Galactic star cluster CR model as the second galactic component. For the star cluster component, the considered injection fraction is ~ 5%, and the cutoff is at $7 \times 10^7 Z$ GeV. The thick dashed maroon line represents the total SNR-CRs, the thick solid maroon line represents star cluster CRs, the thick maroon dotted line represents the UFA model of extragalactic CR component (EG-UFA) [25], and the thick solid blue line represents the total all-particle spectrum. The thin lines represent the total spectra for the individual elements i.e., a combination of both SNR-CR and the CRs originating from star clusters.

the 'ankle' to reproduce the observed CR energy spectrum. With these two models (SNR-CRs & extragalactic CRs), we have combined our proposed star cluster model with a proton spectrum cut-off at 7×10^7 GeV. The cumulative contributions from these three components effectively account for the observed features observed in the all-particle spectrum. Also, the spectra of the individual elements can be explained well with the model.

For comparison with the theoretical predictions, $\langle \ln A \rangle$, the mean logarithmic mass of the measured cosmic rays, is of utmost importance. We calculate the mean mass as follows,

$$\langle \ln\ A \rangle = \frac{\sum_i \ln\ A_i \times \mathrm{Flux_i}}{\sum_i\ \mathrm{Flux_i}}\ . \tag{7}$$

Figure 3 shows that the results obtained using our star cluster model (green curve) follow the observed trend for the mean logarithmic mass in the total energy range from 10^8 GeV to 10^{11} GeV when combined with the UFA model for the extragalactic CRs. In the energy range of about 2×10^7 and 10^8 GeV, our prediction shows some deviation from the observed trend but still lies within limits presented in Kampert & Unger [26].

5. Conclusions

In this study, we propose that the 'second Galactic component of cosmic rays' responsible for explaining the observed flux of cosmic rays in the energy range between the 'knee' and the 'ankle' (10^7 GeV to 10^9 GeV) originates from massive star clusters. This component serves as a

PoS(ICRC2023)196

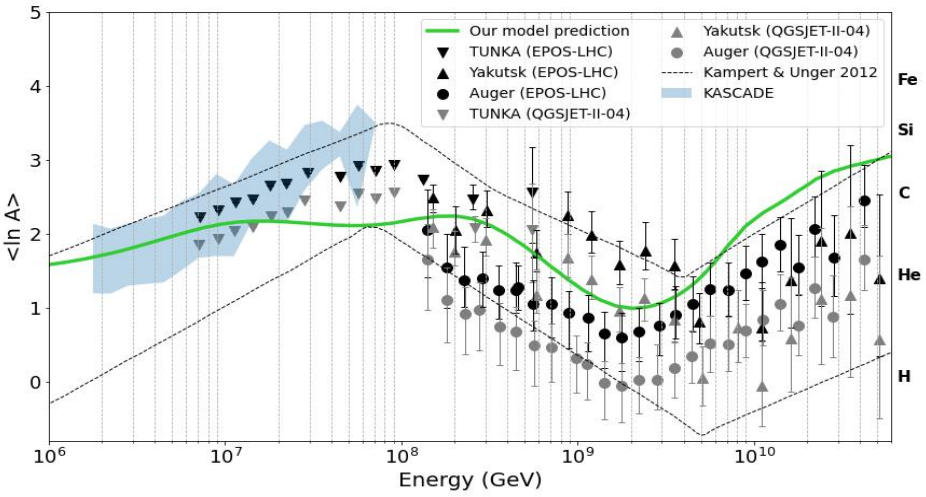

Figure 3: Mean logarithmic mass $\langle \ln A \rangle$ of cosmic rays as a function of energy, predicted using the combination of SNR-CR, CRs from star clusters (these two are Galactic components), and EG-UFA model (extragalactic component, [25]).

bridge between the dominant SNR-CR component, which prevails below approximately 10^7 GeV, and the extragalactic component, which dominates above approximately 10^9 GeV. We have argued that the WTS of massive star clusters can accelerate CRs to a maximum energy of a several tens of PeV, which is larger than that possible in SNR-CRs. In this work, we have carried out a detailed calculation to demonstrate that this model can also fit the all-particle CR spectrum. We consider the observed spatial distribution of star clusters in our Galaxy, as well as all the transport processes of CRs, including re-acceleration by old SNRs.

Our analysis requires a proton cut-off energy of $\sim 7 \times 10^7$ GeV for the CRs accelerated in star clusters, which is consistent with the observed physical conditions in the clusters. A comparison of our analytical results with the observed all-particle CR spectrum yields a reasonable injection fraction of $\sim 5\%$ of the total kinetic energy of the winds.

References

[1] Lagage P. O., Cesarsky C. J., 1983, 125, 249

[2] Axford W. I., 1994, ApJS, 90, 937

[3] Kang, H., Ryu, D., & Jones, T. W., 1996, ApJ, 456, 422

[4] Rachen J. P., Biermann P. L., 1993,A&A 272, 161

[5] Mannheim, K., Protheroe, R. J. and Rachen, J. P., 2001, PRD, 63, 023003

[6] Waxman, E., 1995, PRL, 75, 386

[7] Aharonian, F., Yang, R., Wilhelmi, E. O. 2019 Nature, 3, 561

PoS(ICRC2023)196

[8] Abeysekara A. U., Albert A., Alfaro R., Alvarez C., Camacho J. R. A., Arteaga-Velázquez J. C., Arunbabu K. P., et al., 2021, Nature Astronomy, 5,465

[9] Bykov, A. M. 2014, A & ARv, 22, 77

[10] Gupta, S., Nath, B. B., Sharma, P., Eichler, D., 2020, MNRAS, 493, 3159

[11] Tatischeff V., Raymond J. C., Duprat J., Gabici S., Recchia S., 2021, MNRAS, 508, 1321

[12] Longmore S. N., Kruijssen J. M. D., Bastian N., Bally J., Rathborne J., Testi L., Stolte A., et al., 2014. Protostars and Planets VI, 914, 291

[13] Weaver R., McCray R., Castor J., Shapiro P., Moore R., 1977 ApJ, 218, 377

[14] Webb G. M., Axford W. I., Forman M. A., 1985, ApJ, 298,684

[15] Gupta, S., Nath, B. B., Sharma, P., 2018, MNRAS, 479, 5220

[16] Bykov A. M., Marcowith A., Amato E., Kalyashova M. E., Kruijssen J. M. D., Waxman E., 2020, SSRv, 216,42

[17] Cao Z., Aharonian F. A., An Q., Axikegu B., Bai Y. X., Bao Y. W., Bastieri D., et al., 2021, Nature, 594,33

[18] Thoudam S., Hörandel J. R., 2014, A&A, 567, A33

[19] Bronfman L., Casassus S., May J., Nyman L.-Å., 2000, A&A 358,521

[20] Nath B. B., Eichler D., 2020, MNRAS Letter, 499,L1

[21] Vieu T., Reville B., Aharonian F., 2022, MNRAS, 2256-2265

[22] Hillas A. M., 1984, ARA&A,, 22,425

[23] Thoudam S., Rachen J. P., van Vliet A., Achterberg A., Buitink S., Falcke H., Hörandel J. R., 2016, A&A, 523, L61

[24] Roy A., Dopita M. A., Krumholz M. R., Kewley L. J., Sutherland R. S., Heger A., 2021, MNRAS, 502,4359

[25] Unger M., Farrar G. R., Anchordoqui L. A., 2015, PRD, 92,12

[26] Kampert K.-H., Unger M., 2012, Astroparticle Physics, 35,660

[27] Amenomori M., Bi X. J., Chen D., Cui S. W., Danzengluobu, Ding L. K., Ding X. H., et al., 2008, ApJ, 678,1165

[28] Schulz, A., for the Pierre Auger Collaboration 2013, in Proc. 33rd ICRC, 2013, , arXiv

[29] Abbasi R. U., Abu-Zayyad T., Al-Seady M., Allen M., Amann J. F., Archbold G., et al., 2009, APh, 32,53

[30] Aartsen M. G., Abbasi R., Abdou Y., Ackermann M., Adams J., Aguilar J. A., Ahlers M., et al., 2013, PhRvD, 88,042004

PoS(ICRC2023)196